Calcium isotopes in scleractinian fossil corals since the Mesozoic: implications for vital effects and biomineralization through time

Anne M. Gothmann*[1], Michael L. Bender[1], Clara L. Blättler[1], Peter K. Swart[2], Sharmila J. Giri[2], Jess F. Adkins[3], Jarosław Stolarski[4], John A. Higgins[1]

[1]Princeton University, Department of Geosciences, Princeton, NJ
[2]University of Miami, Department of Marine Geosciences, Miami, FL
[3]California Institute of Technology, Division of Geological and Planetary Sciences, Pasadena, CA
[4]Institute of Paleobiology, Polish Academy of Sciences, Warsaw, Poland

*Corresponding author, *email: gothmann@uw.edu*

Abstract

We present a Cenozoic record of $\delta^{44/40}Ca$ from well preserved scleractinian fossil corals, as well as fossil coral $\delta^{44/40}Ca$ data from two time periods during the Mesozoic (84 and 160 Ma). To complement the coral data, we also extend existing bulk pelagic carbonate records back to ~80 Ma. The same fossil corals used for this study were previously shown to be excellently preserved, and to be faithful archives of past seawater Mg/Ca and Sr/Ca since ~200 Ma (Gothmann et al., 2015). We find that the $\delta^{44/40}Ca$ compositions of bulk pelagic carbonates from ODP Site 807 (Ontong Java Plateau) and DSDP Site 516 (Rio Grande Rise) have not varied by more than ~ ±0.20 ‰ over the last ~80 Myr. In contrast, the $\delta^{44/40}Ca$ compositions of Mesozoic and Early Cenozoic fossil corals are ~1‰ lighter than those of modern corals.

The observed change in coral $\delta^{44/40}Ca$ does not likely reflect secular variations in seawater $\delta^{44/40}Ca$. Instead, we propose that it reflects a vital effect of calcification – specifically, a sensitivity of coral Ca isotope discrimination to changing seawater [Ca] and/or pH. Support for this hypothesis comes from the presence of an empirical correlation between our coral $\delta^{44/40}Ca$ record and records of seawater [Ca] and pH since the Mesozoic (Lowenstein et al. 2003; Hönisch et al. 2012). We explore various mechanisms that could give rise to such a vital effect, including: (1) changes in calcification rate, (2) changes in proton pumping in exchange for Ca^{2+}, (3) variable Rayleigh distillation from an isolated calcifying fluid, and (4) changes in the calcium mass balance of the extracellular calcifying fluid (termed here the "leaky Ca model"). We test for the dependence of seawater $\delta^{44/40}Ca$ on external seawater [Ca] by measuring the $\delta^{44/40}Ca$ of cultured corals grown in seawater solutions with [Ca] ranging from 10 to 15

mmol/kg. Corals grown under elevated [Ca] conditions show a slight, ~0.15‰ depletion of $\delta^{44/40}$Ca at higher seawater [Ca] – a supportive but not definitive result.

Keywords

Ca isotopes; scleractinian coral; vital effects; bulk carbonate; culture experiment; seawater chemistry

1. Introduction

Diagenetically unaltered scleractinian fossil corals are useful archives of paleoenvironmental properties across a range of geologic timescales. For example, coral-based paleothermometers (Sr/Ca, $\delta^{18}O$) have been applied to reconstruct high-resolution records of past climate (e.g., Corrège, 2006; Gaetani et al. 2011). Fossil corals have also been used to reconstruct the geochemical evolution of seawater (i.e., seawater Mg/Ca and Sr/Ca) on timescales of millions of years (Gothmann et al., 2015). The application of corals as paleoenvironmental indicators, however, can sometimes be confounded by the presence of 'vital effects' (Corrège, 2006; Gaetani et al. 2011).

'Vital effects' refer to departures in skeletal geochemistry away from the composition expected based on inorganic distribution coefficients, and they are thought to result from biological control by the coral organism over skeletal calcification (Weiner and Dove, 2003). Problematically, they may also vary between and within coral species, in which case constant correction factors cannot be employed (Weiner and Dove, 2003; Corrège, 2006; Gaetani et al. 2011).

The existence of vital effects in scleractinian coral has been very well documented, but a full mechanistic understanding of their origin has yet to be achieved (Weiner and Dove, 2003). Mechanisms that have been identified as potential sources of vital effects include, but are not limited to (1) Rayleigh fractionation from an isolated calcifying fluid and/or other reservoir effects (e.g., Gaetani et al., 2011), (2) biologically-mediated ionic transport into the calcifying space (e.g., Böhm et al., 2006), (3) variable calcification rates (e.g., as discussed in Corrège, 2006) and (4) the influence of an organic matrix (e.g., Weiner and Dove, 2003).

Existing measurements of $\delta^{44/40}$Ca in modern corals suggest the presence of significant vital effects for Ca isotopes. Modern coral $\delta^{44/40}$Ca is on average ~0.4 ‰ heavier than inorganic aragonite (Chang et al., 2004; Böhm et al., 2006; Pretet et al., 2013; Inoue et al. 2015). For reference, inorganic aragonite is offset from seawater by about -1.7 ‰ (Blättler et al., 2012; Gussone et al., 2003). In addition, modern corals exhibit a ~0.4 ‰ range in $\delta^{44/40}$Ca compositions (Böhm et al., 2006; Blättler et al., 2012; Pretet et al., 2013; Inoue et al. 2015). This range cannot be attributed to variations in coral taxonomy, changes in salinity, or temperature.

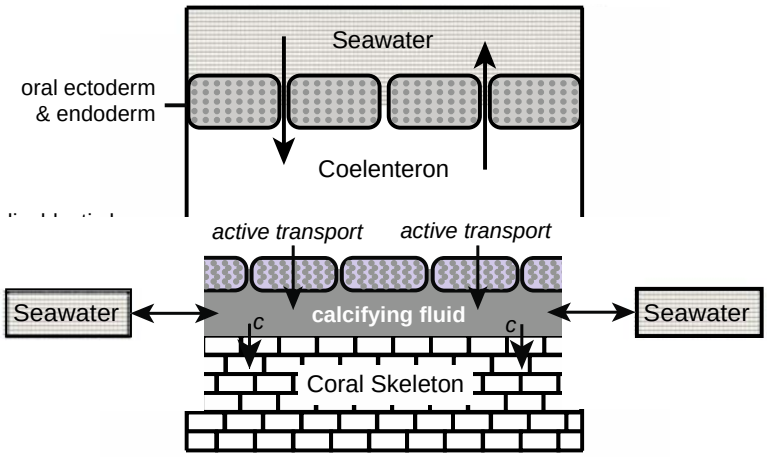

Figure 1. Sketch of key skeletal compartments and reservoirs that play a role in coral calcification, modified from Böhm et al. (2006). Seawater transport to the site of calcification can occur via direct exchange, or can occur transcellularly by active transport with Ca-ATPase. The label 'c' denotes arrows marking calcification.

Ca isotopes may offer unique insight into the mechanisms driving coral vital effects because calcium plays a critical role in calcification. There are two main pathways by which Ca may arrive at the site of coral calcification (Fig. 1). First, Ca^{2+} that has diffused into the coelenteron (the mouth of the coral animal) may be actively transported

87 by Ca-ATPase to the site of calcification (e.g., Al-Horani et al. 2003). There are also
88 suggestions that seawater may be transported paracellularly (i.e., via open channels or
89 conduits) directly to the site of calcification (e.g., Tambutté et al. 2011). The calcification
90 site may exist as a thin, seawater-like "calcifying fluid" beneath the calicoblastic layer
91 (Al-Horani et al. 2003; Gaetani et al. 2011). Alternatively, calcification may occur
92 directly from an organic matrix (e.g., Weiner and Dove, 2003).
93 It is possible that external seawater carbonate chemistry and seawater [Ca]
94 influence each of the abovementioned pathways and the isotope effects associated with
95 them. Ca isotope fractionation in inorganic calcite and aragonite precipitated from
96 aqueous solutions has been found to depend on calcification rate (Lemarchand et al.,
97 2004; Tang et al., 2008; Gussone et al., 2003), which in turn has been shown to depend
98 on the $[CO_3^{2-}]/[Ca^{2+}]$ ratios of natural waters (Nielsen and DePaolo, 2013). Rayleigh
99 distillation (e.g., Gaetani et al., 2011) may also lead to a dependence of Ca isotope
100 discrimination on seawater [Ca]. Another possibility is that coral Ca isotope fractionation
101 is dependent on seawater [Ca] in a way similar to the dependence of carbon isotope
102 fractionation on pCO_2 in plants. In plants cells, the ratio of carbon fixation by the enzyme
103 RuBisCO, relative to the amount of CO_2 that diffuses back to the surrounding
104 environment, is dependent on pCO_2. Because the isotope effects associated with fixation
105 and diffusion are distinct, the degree of carbon isotope fractionation expressed also
106 depends on pCO_2 (Pagani, 2014). Likewise, in coral, the ratio of Ca that is incorporated
107 into coral aragonite from the calcifying fluid, relative to the amount of Ca returned to
108 seawater, may be dependent on external seawater [Ca].

Böhm et al. (2006) hypothesize that Ca isotope fractionation in coral results, at least in part, from active biologically-mediated transport of Ca^{2+} to the site of calcification. As a result, changes in seawater [Ca] could presumably affect the proportion of Ca in the coral skeleton derived from active pumping by Ca-ATPase relative to Ca derived from a direct seawater pathway. As suggested by Gagnon et al. (2013), seawater pH, alkalinity and saturation state may also play a role in setting the proportion of skeletal Ca that comes directly from seawater, relative to the amount derived from Ca-ATPase. Studies of boron isotopes and pH-sensitive dyes in coral (McCulloch et al. 2012; Venn et al., 2013) present additional evidence in support of a relationship between proton pumping by Ca-ATPase and seawater carbonate chemistry.

We measured Ca isotopes in a suite of well preserved fossil aragonitic corals (Gothmann et al., 2015), bulk pelagic carbonates from ODP Site 807 and DSDP Site 516, and corals cultured under a range of seawater [Ca]. Collectively, the data allow us to examine how coral Ca isotope fractionation has responded to natural variations in seawater [Ca] and pH since the Mesozoic (Lowenstein et al., 2003; Hönisch et al., 2012). Our results provide new insights into the relationship between coral calcification and secular variations in seawater chemistry over million-year timescales.

2. Materials and methods

2.1 Fossil coral, bulk pelagic carbonate, and cultured coral samples

The fossil coral samples (n=38) studied here were previously screened for diagenetic alteration and described by Gothmann et al. (2015). Fossil corals measured for Ca isotopes are as old as Jurassic in age and have been obtained from a variety of

132 geologic localities to ensure that variations through time reflect global rather than local
133 signatures. While our sample set includes a range of different species of coral, there are
134 no trends in our sample set between coral taxonomy and geologic age. Details of sample
135 taxonomy and provenance are presented in the supplementary materials (Table S1).
136 Bulk pelagic carbonate samples from ODP Site 807 (Ontong Java Plateau,
137 ~2800 m water depth) and DSDP Site 516 (Rio Grande Rise, ~1300 m water depth) were
138 also measured for $\delta^{44/40}$Ca. Samples range in age from Late Cretaceous to Recent. Cores
139 from both sites are generally carbonate-rich, although some intervals of claystone and
140 radiolarian siltstone are also present (Kroenke et al., 1991; Fantle and DePaolo, 2007;
141 Barker et al., 1983). Sediments of Eocene age and younger are dominated by foraminifer
142 oozes, nannofossil oozes, and chalk. Eocene and older sediments are dominated by
143 lithified limestone (Kroenke et al., 1991; Barker et al., 1983). Bulk carbonate samples
144 were washed and sieved prior to geochemical analysis as described in Higgins and
145 Schrag (2015).
146 Cultured coral samples were grown for 9 weeks under controlled laboratory
147 conditions at the University of Miami's Experimental Hatchery. Concentrations of
148 calcium in the culture solutions were varied to assess the effect of past changes in
149 seawater [Ca] on coral Ca isotope discrimination. Calcium concentrations of the growth
150 solutions ranged from modern seawater concentrations (~10 mmol/kg) to concentrations
151 similar to those expected for the late Oligocene or Early Miocene (~15 mmol/kg)
152 (Lowenstein et al., 2003). (For reference, Early Cenozoic seawater [Ca] was ~25-30
153 mmol/kg, 250-300% of present: Lowenstein et al., 2003). While some colonies were only
154 subjected to elevated [Ca], others were also subjected to elevated [Mg] and [Sr].

Prior to starting experiments, 2 branches (>1.5 cm in length) of *Pocillopora damicornis* were fragmented from coral colonies using wire cutters. These fragments were then glued to PVC tiles with CorAffix^{TM} Cyanoacrylate Adhesive and allowed to recover for 4 weeks in flow-through seawater. Seawater was pumped from Bear Cut, a tidal channel that connects Biscayne Bay to the Atlantic Ocean. The composition of this water varied naturally each day. Temperature ranged from 21-25°C, with an average of 22.6°C, and salinity ranged from 31-35 psu, with an average of 34 psu. The average alkalinity for the experiments was 2.261 ± 0.061 meq/kg (1σ S.D.) and pH varied between 7.9-8.0.

The start of the experiment was marked with Alizarin Red S biological stain after which fragments were moved to jars with 2.5 L of seawater. Concentrations of Ca, Mg and Sr were increased incrementally in the seawater solutions over 24 hours by adding calcium, magnesium, and strontium chloride salts. Flow was maintained in these jars with aquarium pumps and seawater treatments were changed daily. Coral tissues were removed from skeletons with an airbrush, and skeletons were oven dried at 40°C for 24 hours. Areas of new growth (above the Alizarin stain line) were ground to a powder for Ca isotope analysis. Culture seawater solutions were also collected, filtered, and analyzed for $\delta^{44/40}$Ca. For additional detail regarding coral culture experiments, calculation of calcification rates, and saturation state, the reader is referred to the supplementary text.

178 **2.2 Ca isotope analyses**

179 Powders weighing 2-5 mg were drilled from fossil coral skeletons and
180 dissolved in 1N nitric acid (HNO_3). The majority of fossil coral powders contain ≤1%
181 calcite as determined by X-ray diffractometry (Gothmann et al. 2015). However, a small
182 number of specimens contain between 2% and 8% calcite as noted in Table 1. For
183 cultured coral samples, ~100 μg of $CaCO_3$ was dissolved in 1 mL 1N HNO_3. Bulk
184 carbonate samples (~5 mg) were powdered and dissolved in buffered 0.1N acetic acid
185 (pH ≈ 5) to dissolve carbonate phases. Ca in dissolved carbonates and culture seawater
186 solutions was purified by ion exchange chromatography as described in Blättler et al.
187 (2012) and Blättler and Higgins (2014), and also using a Thermo Dionex DCS5000+ Ion
188 Chromatograph (IC). The IC system offers a more efficient means (30-50 minute
189 separation per sample) by which to separate and collect cations such as Ca for isotopic
190 analysis.

191 Samples were prepared for separation on the IC by diluting to ~30 ppm Ca
192 with 0.2% HNO_3. Samples (200 μL in volume) were then injected, and Ca was separated
193 from other cations (Na, Mg, K, Sr) using an in-line CS16 cation exchange column. After
194 eluting with methanesulfonic acid (MSA), Ca fractions were collected using a Dionex
195 AS-AP autosampler. Cation separation and yields were verified by measurements of
196 sample conductivity. Sample conductivity was also monitored in 0.2% HNO_3 solutions
197 used for diluting samples in order to ensure that procedural blanks were <1%. Accuracy
198 and precision of the method were assessed by repeated measurements of carbonate
199 standards (in-house and SRM 915b) and modern seawater standards.

Separated Ca fractions were analyzed for Ca isotopes (44/42, 44/43, 43/42) at a concentration of 2 ppm Ca. Measurements were made using a ThermoFinnegan Neptune Plus inductively-coupled plasma mass spectrometer (ICP-MS) at Princeton University with an ESI Apex-IR sample introduction system. Beam intensities were measured in medium resolution for masses 44, 43 and 42. Mass 43.5 was also monitored to check for Sr interferences. Three-isotope plots of $\delta^{44/43}$ vs. $\delta^{44/42}$ for each analytical session were examined to check for mass-dependent behavior. Raw $\delta^{44/42}$Ca results were converted to $\delta^{44/40}$Ca and calibrated relative to modern seawaters measured in the same analytical session (i.e., $\delta^{44/40}Ca_{\text{modern seawater}} = 0$ by definition).

The $\delta^{44/40}$Ca of an in-house Ca standard, taken through the full chemical procedure with each batch of samples in order to monitor long-term external reproducibility, is -1.11 ± 0.18‰ (2 S.D.; n=14) relative to modern seawater. Measurements of SRM 915b yield $\delta^{44/40}$Ca values of -1.18 ± 0.18‰ (2 S.D.; n=11) relative to modern seawater, indistinguishable from values reported in previous studies as measured by MC-ICP-MS (-1.16‰: Morgan et al. 2011) and by thermal ionization mass spectrometry (TIMS) (-1.12 ‰ and -1.13‰: Heuser and Eisenhauer, 2008 and Lehn et al., 2013). A modern *Porites* sp. coral gives a $\delta^{44/40}$Ca value of -1.01 ± 0.13‰ (2 S.D.; n=3) relative to modern seawater – within the range of values measured for other modern *Porites* sp. (Pretet et al., 2013).

3. Results

Results of $\delta^{44/40}$Ca measurements in modern and fossil corals are given in Table 1 and Fig. 2. We measure $\delta^{44/40}$Ca compositions in modern and Late Pleistocene corals ranging from -1.24 ‰ to -1.01 ‰ (vs. modern seawater), consistent with previous studies (Chang et al., 2004; Pretet et al., 2013; Böhm et al., 2006; Inoue et al. 2015; Blättler et al., 2012). Ca isotope compositions measured in fossil corals become systematically lighter with increasing geologic age (Fig. 2). Jurassic age samples exhibit the lightest Ca isotope compositions with an average of -2.16 ‰, which is approximately 1‰ lighter than the $\delta^{44/40}$Ca measured for modern corals. The apparent Jurassic coral $\delta^{44/40}$Ca offset from modern seawater also exceeds the inorganic aragonite fractionation factor of -1.7 ‰ (Blättler et al., 2012; Gussone et al., 2003). Using the average apparent fractionation between our modern coral samples and modern seawater, we convert fossil coral $\delta^{44/40}$Ca to seawater $\delta^{44/40}$Ca values (Fig. 2a and 2b – see left-hand axis). As imposed by our applied offsets, our inferred modern seawater $\delta^{44/40}$Ca value from coral overlaps with $\delta^{44/40}$Ca compositions inferred from other archives (Fig. 2a and 2b). However, the fossil coral record departs from other records going back in time to the Mesozoic. For example, our Mesozoic data are highly divergent from the Farkaš et al. (2007) record reconstructed from brachiopods, belemnites, and rudists (Fig. 2a).

Table 2 and Fig. 2c give results of $\delta^{44/40}$Ca measurements in bulk pelagic carbonates from ODP Site 807 and DSDP Site 516. Our bulk pelagic carbonates are normalized to modern samples using an offset of ~1.2‰. This number was chosen based on our Site 807 results (Table 2) and data in Fantle and DePaolo (2007). Our bulk pelagic carbonate record is in good agreement with other pelagic carbonates from ODP Site 807

and DSDP Site 590 (Fantle and DePaolo, 2005; Fantle and DePaolo, 2007). In contrast with fossil corals, which show a large change in $\delta^{44/40}$Ca with time, our record of bulk carbonate $\delta^{44/40}$Ca shows variability of ~ ±0.20 ‰ over the last 80 Myr (Fig. 2c), with an average $\delta^{44/40}$Ca of -1.32 ± 0.2 ‰ (2σ S.D; n=47). We also observe a minimum in the $\delta^{44/40}$Ca of bulk carbonate at ~35 Ma.

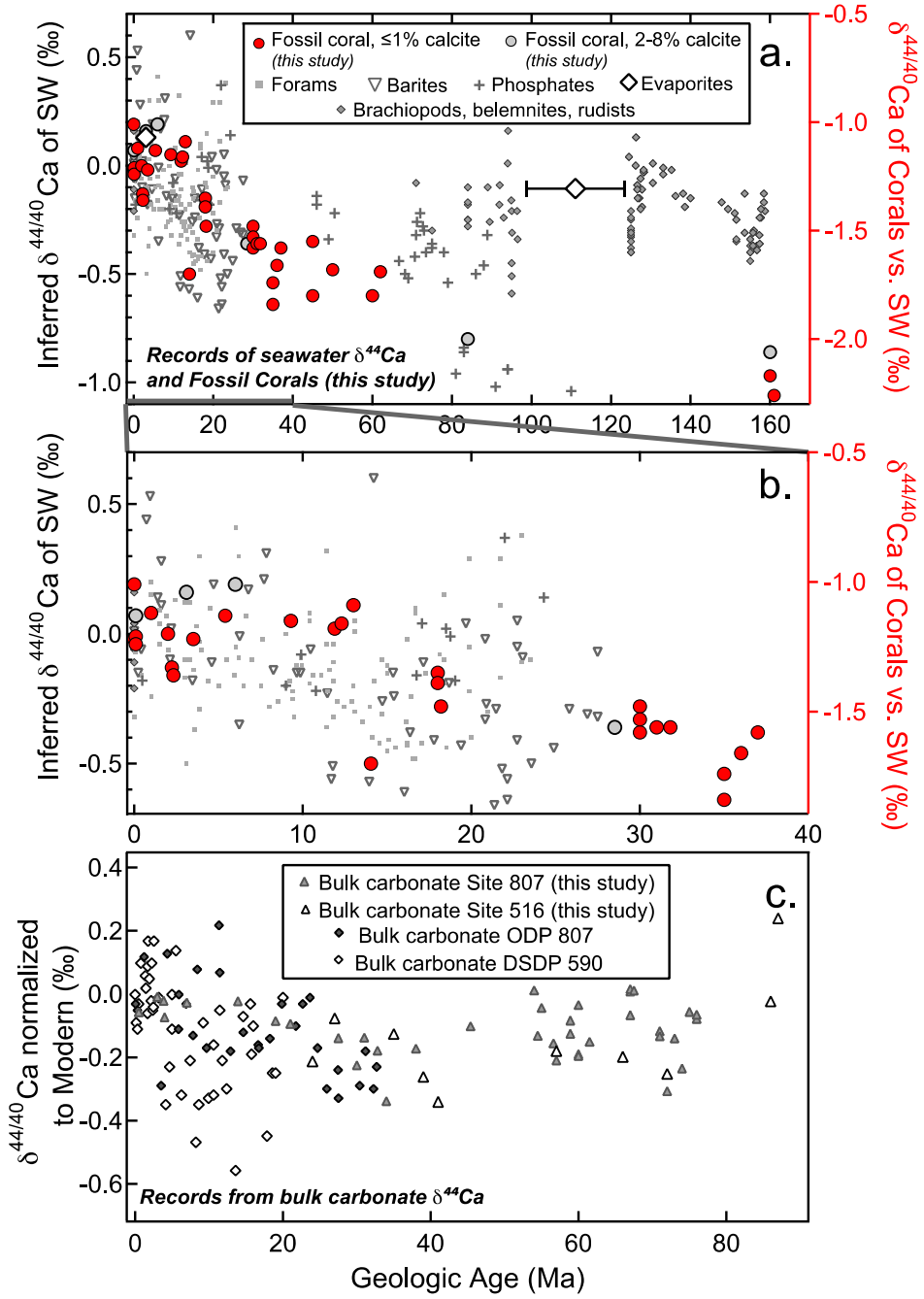

Figure 2. Records of inferred seawater, fossil coral, and bulk pelagic carbonate Ca isotopes. (a) Records of inferred seawater $\delta^{44/40}$Ca vs. time including our record from fossil corals. Evaporite data are from Blättler and Higgins, (2014); brachiopods, belemnites and rudists are from Farkaš et al. (2007) and Steuber and Buhl (2006); phosphate data are from Soudry et al. (2004), Soudry et al. (2006) and Schmitt et al. (2003); barite data are from Griffith et al. (2008); foraminifera data are from Sime et al. (2007) and Heuser et al. (2005). (b) Same as in (a), but enlarged to show only the last 40 Myr. Uncertainties in fossil coral $\delta^{44/40}$Ca are listed in Table 1. Before the Late Eocene,

fossil corals disagree with other archives, with the exception of authigenic phosphates. The left-hand axis gives inferred seawater $\delta^{44/40}$Ca compositions. The right-hand axis gives measured coral $\delta^{44/40}$Ca vs. modern seawater. (c) Records of bulk carbonates from this study (ODP Site 807 and DSDP Site 516), Fantle and DePaolo (2005), and Fantle and DePaolo (2007). All records are normalized to modern bulk carbonate samples.

Table 1. Results of Ca isotope analyses in Recent and fossil corals. Uncertainties are reported as 2σ S.D. where the number of replicate analyses (n) is = 2, and 2σ S.E. where n > 2. Ages are based on $^{87}Sr/^{86}Sr$ isotope compositions or best estimates of the age of the geologic formation from which samples are collected as detailed in Gothmann et al. (2015).

Sample Name	Estimated Age (Ma)	$\delta^{44/40}$Ca vs. SW	2σ S.D./S.E.	n
ERP	0	-1.01	0.07	3
M1	0	-1.22	0.02	2
Pl3	0.1	-1.21	0.01	3
Pl4	0.1	-1.24	0.10	2
Pl5*	0.1	-1.13	0.11	3
Pl2	1	-1.12	0.16	3
Pl7	2	-1.20	0.14	3
Pl8	2	-1.33	0.13	3
Pli3	2.3	-1.36	0.10	3
Pli2*	3.1	-1.04	0.14	2
Pli1	3.5	-1.22	0.06	2
Mi6	5.4	-1.13	0.04	2
Mi9*	6	-1.01	0.09	3
Mi11	9	-1.15	0.05	4
Mi13	11.9	-1.18	0.06	3
Mi16	12.3	-1.16	0.06	3
Mi14	13.0	-1.09	0.19	3
Mi7	14	-1.70	0.15	3
Mi2	18.0	-1.35	0.29	2
Mi1	18	-1.39	0.16	3
Mi3	18.2	-1.48	0.03	3
Ol1*	28.5	-1.56	0.12	3
Ol5	30.0	-1.48	0.11	3
Ol6	30	-1.58	0.12	2
Ol4	30	-1.53	0.21	2
Ol2	31	-1.56	0.07	3
Ol3	31.8	-1.56	0.07	2
E6	35.0	-1.84	0.01	2
E1	35	-1.74	0.06	2
E8	36	-1.66	0.17	2
E2	37	-1.58	0.19	3
E5	45	-1.55	-	1
E4	45	-1.80	0.16	2
E3	50	-1.68	0.20	3
Pa1	60	-1.80	0.23	3
Pa3	62	-1.69	0.21	3
K3*	84	-2.00	0.05	3
J1	160	-2.17	0.14	3
J2*	160	-2.06	0.04	2
J4	161	-2.26	0.04	2

* Samples with 2-8% calcite in powders used for Ca isotope analyses. All other samples have ≤1% calcite.

Table 2. Results of Ca isotope analyses on bulk carbonates from deep sea sediments. Ages are based on biostratigraphic markers at the depth from which the sample was collected (Barker et al. 1983; Kroenke et al. 1991). Uncertainties are reported as 2σ S.D. where the number of replicate analyses (n) is = 2, and 2σ S.E. where n > 2.

Sample Name	Depth (mbsf)	Age (Ma)	$\delta^{44/40}$Ca vs. SW	2σ S.D./S.E	n	Notes
807A-2W-2H	7-16.9	0.5	-1.26	-	1	ooze
807A-3-4H	27.35-35.5	3	-1.20	0.09	3	ooze
807A-3W-11H	92-102	3.86	-1.22	0.09	2	ooze
807A-2-9H	74.25-83.25	4	-1.25	0.07	2	ooze
807A-2-21H	188.9-197.0	7	-1.23	0.12	2	ooze
807A-5W-42X	389-399	13.9	-1.26	0.12	2	chalk
807A-3W-50X	467.3-474.9	19	-1.28	0.03	2	chalk
807A-6W-53X	495-505	21	-1.28	0.02	2	chalk
807A-2W-72X	678.2-687.8	27.5	-1.42	0.23	2	chalk
807A-1W-84X	793-803	32.8	-1.36	0.04	2	chalk
807C-1W-2R	789-799	30	-1.39	0.11	2	chalk
807C-2W-6R	828-838	31	-1.36	0.07	2	chalk
807C-1W-17R	904.2-905.9	34	-1.44	0.28	2	chalk
807C-1W-25R	948-958	38	-1.41	0.11	2	chalk
807C-1W-38R	1073-1082	45.4	-1.25	0.16	2	chalk
807C-1W-42R	1101-1106	54	-1.19	0.12	3	limestone
807C-1W-44R	1116-1125	54.5	-1.33	0.18	3	limestone
807C-2W-46R	1135-1140	55	-1.24	0.13	3	limestone
807C-2W-48R	1145-1150	56.6	-1.36	0.10	3	limestone
807C-1W-50R	1155-1160	57	-1.41	0.02	3	limestone
807C-1W-51R	1160-1169	58.9	-1.28	0.13	2	limestone
807C-2W-51R	1160-1170	58.9	-1.32	0.07	2	limestone
807C-1W-52R	1169-1178	60	-1.23	-	1	limestone
807C-2W-52R	1169-1179	60	-1.39	0.09	3	limestone
807C-4W-52R	1169-1180	60	-1.37	0.11	3	limestone
807C-2W-53R	1179-1188	61.5	-1.35	0.07	2	limestone
807C-2W-54R	1188-1196	67	-1.27	0.15	2	limestone
807C-3W-54R	1188-1197	67	-1.19	0.13	3	limestone
807C-4W-54R	1188-1198	67	-1.20	0.11	3	limestone
807C-1W-55R	1196-1206	67.5	-1.17	0.15	3	limestone
807C-2W-61R	1251-1261	71	-1.32	0.16	3	limestone
807C-2W-62R	1261-1270	71	-1.33	0.08	3	limestone
807C-2W-63R	1270-1280	72	-1.51	0.20	3	limestone
807C-1W-65R	1290-1299	73	-1.34	0.06	3	limestone
807C-1W-67R	1309-1319	74	-1.44	0.07	3	limestone
807C-2W-69R	1328-1338	75	-1.25	0.15	3	limestone
807C-2W-70R	1338-1348	76	-1.28	0.10	3	limestone
807C-1W-71R	1348-1357	76	-1.27	0.11	3	limestone/claystone
516F-15-6	310-311.6	24	-1.41	0.02	2	chalk
516F-20-4	354-356	27	-1.28	0.19	2	chalk
516F-45-1	587.1-596.6	35	-1.33	0.08	2	chalk
516F-50-2	636.1-637.6	39	-1.46	0.07	2	limestone
516F-55-1	682.1-691.6	41	-1.54	0.17	2	limestone
516F-83-1	900.6-910.1	57	-1.38	0.12	2	limestone
516F-90-2	967.1-976.6	66	-1.40	0.19	2	limestone
516F 98-2	1032.6-1041.1	72	-1.43	0.12	3	limestone
516F-117-3	1184.1-1185.5	86	-1.22	0.09	3	limestone

4. Discussion

There are three possible explanations for the apparent divergence between our coral record and other $\delta^{44/40}Ca$ records during the Mesozoic and Early Cenozoic. Fossil coral $\delta^{44/40}Ca$ could reflect (1) progressive diagenetic alteration with increasing sample age, (2) variations in seawater $\delta^{44/40}Ca$ driven by changes in the average fractionation of the main seawater Ca sink ($CaCO_3$), or (3) changes in coral Ca isotope discrimination over time. In other words, if all of the records reflect primary geochemistry, there must either have been a change in the isotope effect of corals, or a change in the isotope effect associated with the rest of the carbonate sink (as recorded by pelagic carbonates). We show that explanations (1) and (2) are improbable, and then discuss possible mechanisms for (3) in the context of changes in the major element and carbonate chemistry of seawater since the Mesozoic. We conclude that changes in seawater [Ca] and/or pH may have an effect on coral Ca isotope discrimination.

4.1 Fossil coral and bulk pelagic carbonate preservation

It is not plausible to explain the observed trend in fossil coral $\delta^{44/40}Ca$ by invoking progressive diagenetic alteration of samples. The fossil coral samples analyzed here for $\delta^{44/40}Ca$ were previously screened for alteration by Gothmann et al. (2015) and shown to be extremely well preserved. Techniques used to test for mineralogical changes indicative of diagenesis include X-ray diffractometry, scanning electron microscopy, petrographic microscopy, cathodoluminescence, and micro-raman. Tests used to constrain preservation of sample geochemistry include measurements of $^{87}Sr/^{86}Sr$ isotopes, carbonate clumped isotopes, and trace elements sensitive to diagenesis (e.g.,

301 Mn/Ca). These corals have also been found to faithfully record other properties of
302 seawater chemistry (Mg/Ca, Sr/Ca: Gothmann et al., 2015). It is difficult to conceive how
303 the trace element composition of these fossil coral samples could be retained, while the
304 isotopic composition of Ca, which makes up 40% of coral $CaCO_3$ by mass, is altered.
305 Moreover, diagenesis in platform carbonates shifts $\delta^{44/40}$Ca toward heavier values (Fantle
306 and Higgins, 2014). Instead, we observe a shift to lighter coral $\delta^{44/40}$Ca with increasing
307 age.

308 Another concern associated with fossil coral preservation has to do with older
309 samples being biased toward restricted marine environments or epicontinental seas
310 because of a higher likelihood of preservation. Holmden et al. (2012) showed that high
311 [Ca] and low $\delta^{44/40}$Ca of submarine groundwaters are responsible for driving a 0.7 ‰
312 gradient in seawater $\delta^{44/40}$Ca in the Florida Bay. This result suggests that, going forward
313 in time, a shift between samples from restricted marine environments to samples obtained
314 from open marine environments, could drive changes of the magnitude we observe. This
315 explanation, however, seems unlikely considering that our data show a monotonically
316 increasing trend, with no change in the spread of the data with time. For example, the
317 average $\delta^{44/40}$Ca of modern and Pleistocene samples is -1.18 ± 0.19 ‰ and the average
318 $\delta^{44/40}$Ca of Eocene and Paleocene samples is -1.7 ± 0.20 ‰. In addition, while samples
319 from the Mesozoic are all from the paleo-Tethys region, potentially raising concerns
320 about regional biases, samples from the Eocene and Paleocene, were collected from a
321 broad range of geologic localities (see Table S1), limiting the potential for local effects.

322 It is also unlikely that our bulk carbonate $\delta^{44/40}$Ca record is reflective of
323 sedimentary diagenesis. The amount of isotopically heavy seawater Ca incorporated into

bulk carbonates during diagenesis is diffusion-limited (Fantle and DePaolo, 2007; Fantle et al., 2010). Both ODP Site 807 and DSDP Site 516 sediments range from 75 to >90 wt % carbonate (Barker et al., 1983; Kroenke et al., 1991), suggesting that pore fluids at both sites are buffered by the high Ca content of the sediments. In other words, recrystallization does not cause the Ca isotope composition of $CaCO_3$ to change because the flux of "new" Ca to the sediments is small compared to the sedimentary Ca mass. Indeed, Fantle and DePaolo (2007) modeled pore fluid and sediment geochemistry at ODP Site 807 and calculated maximum diagenetic shifts in carbonate $\delta^{44/40}$Ca of 0.1 to 0.15‰, which is similar to our measurement uncertainty.

4.2 The seawater Ca isotope mass balance

One possible explanation for the divergent coral and pelagic carbonate records is that the coral record, rather than the sedimentary carbonate record, may accurately reflect changes in the Ca isotopic composition of seawater through time (i.e., that corals passively record seawater composition and there was a 1 ‰ increase in seawater $\delta^{44/40}$Ca between the Mesozoic and present). Existing records of $\delta^{44/40}$Ca can be considered using a simple steady-state Ca isotope mass balance:

$$\delta^{44/40}Ca_{input} = \delta^{44/40}Ca_{output} = \delta^{44/40}Ca_{seawater} - \varepsilon \,, \qquad \text{(Eqn. 1)}$$

where $\delta^{44/40}Ca_{input}$ represents the Ca isotopic composition of the main source of Ca to seawater (rivers), $\delta^{44/40}Ca_{output}$ represents the Ca isotopic composition of the main sink of Ca from seawater ($CaCO_3$), $\delta^{44/40}Ca_{seawater}$ is the Ca isotopic composition of seawater, and

ε is the globally averaged fractionation factor for the seawater Ca sink (De La Rocha and DePaolo, 2000; Blättler et al., 2012; Fantle and Tipper, 2014). This mass balance indicates that, on timescales longer than the Ca residence time (~10^6 years), changes in $\delta^{44/40}Ca_{seawater}$ can result either from changes in the isotopic composition of Ca inputs (from rivers) or from changes in the average ε of the seawater Ca sink.

Because pelagic carbonates are thought to constitute a large fraction of the modern seawater Ca sink (>55% according to Milliman, 1993), our bulk pelagic $\delta^{44/40}Ca$ record can provide a constraint on $\delta^{44/40}Ca_{output}$, and thus $\delta^{44/40}Ca_{input}$ as well (Eqn. 1). For reference, corals may represent ~20% of the total $CaCO_3$ sink according to Milliman (1993), and this percentage has likely varied with time. Our bulk carbonate record indicates that the Ca isotopic composition of the pelagic carbonate sink varied by up to ±0.20 ‰, over the last 80 Myr, with a minimum at ~35 Ma. Records of $\delta^{44/40}Ca$ from brachiopods, belemnites, and rudists (Farkaš et al., 2007) and bulk forams (e.g., Sime et al. 2007; Heuser et al., 2005) show little variability since the Mesozoic as well. As a result, it is unlikely that $\delta^{44/40}Ca_{output}$ shifted by more than 0.3-0.4 ‰ since the Mesozoic. Considering Eqn. 1, then the record also suggests that $\delta^{44/40}Ca_{input}$ has not changed by more than 0.3-0.4 ‰. In Fig. 3a and 3b, we show a simple schematic model to demonstrate the impact of changes in $\delta^{44/40}Ca_{input}$ on $\delta^{44/40}Ca_{seawater}$ and $\delta^{44/40}Ca_{output}$.

Assuming little change in $\delta^{44/40}Ca_{input}$, the only mechanism capable of explaining a ~1‰ change in $\delta^{44/40}Ca_{seawater}$ would be a change in ε of ~1‰ (Eqn. 1; Fig. 3 c and 3d). However, evidence against a ~1‰ change in $\delta^{44/40}Ca_{seawater}$ and ε comes from the Ca isotopic composition of seawater as inferred from $CaSO_4$ evaporites (Fig. 2; Blättler and Higgins, 2014; Farkaš et al., 2007). This archive indicates that seawater

370 $\delta^{44/40}$Ca may have been 0.2-0.3‰ lower during the Cretaceous but does not support a
371 large, >0.5‰ increase in seawater $\delta^{44/40}$Ca. We suggest that small changes in ε could
372 contribute to the discrepancy between the coral and bulk carbonate records. However, it

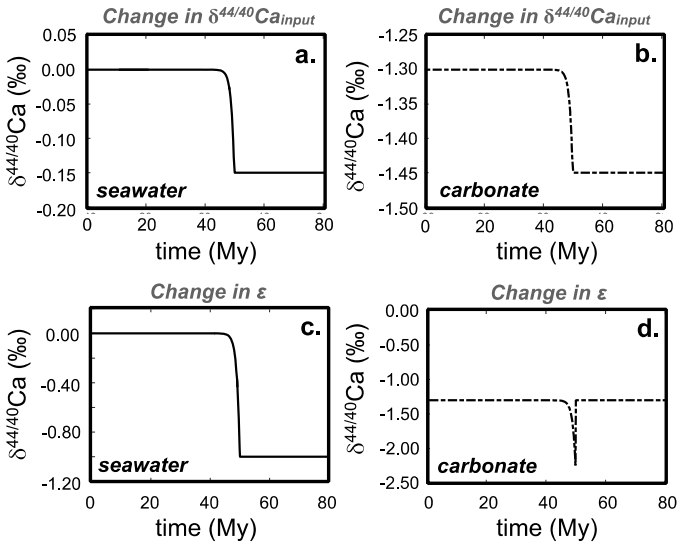

388 Our fossil coral $\delta^{44/40}$Ca record most likely reflects a decrease in coral Ca
389 isotope discrimination since the Mesozoic. Moreover, we propose that this change in
390 coral Ca isotope discrimination results from a response of coral calcification to variations

391 in key seawater carbonate chemistry parameters such as [Ca] and pH. We choose these
392 variables because they empirically correlate with our coral Ca isotope record (Lowenstein
393 et al., 2003; Hönisch et al., 2012), and both play important roles in coral biocalcification
394 (Al-Horani et al., 2003).

395 Assuming the Farkaš et al. (2007) data set provides the most robust current
396 representation of seawater $\delta^{44/40}$Ca since the Mesozoic, we calculate the apparent
397 fractionation between fossil corals and seawater, and plot those results against seawater
398 [Ca] estimated for the time at which each coral grew (see supplementary text for details;
399 Fig. 4). Inferred seawater [Ca] is calculated from a linear interpolation between seawater
400 [Ca] data reconstructed from brine inclusions in halite (e.g., Lowenstein et al. 2003; see
401 supplementary text). The overall magnitude of change in apparent Ca isotope
402 discrimination between modern and Mesozoic corals is ~0.8 ‰.

403 We observe an inverse relationship between apparent coral Ca fractionation
404 and estimated seawater [Ca] at the time of skeletal growth (Fig. 4). Seawater [CO_3^{2-}] and
405 pH also co-vary with [Ca] over this time period (Hönisch et al., 2012; Zeebe et al., 2012),
406 so we cannot exclude the possibility that these geochemical variables may also contribute
407 to the change in apparent Ca isotope fractionation observed.
408

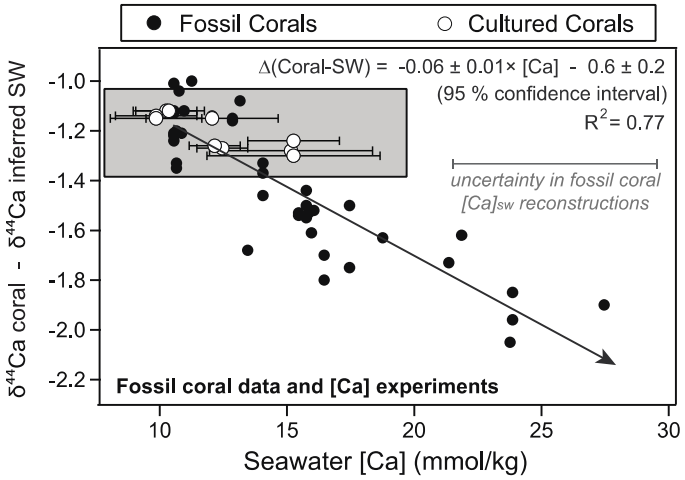

409

410 **Figure 4.** Fossil and cultured coral Ca isotope discrimination against seawater [Ca].
411 Black filled circles correspond to fossil coral samples. Estimates for seawater [Ca]
412 corresponding to each fossil coral sample are derived from reconstructions from fluid
413 inclusions in halite (Lowenstein et al. 2003; see supplementary materials for more detail).
414 White circles correspond to corals grown in culture experiments, which were performed
415 across a range of culture solution [Ca] concentrations. An enlargement of the culture
416 coral data (region corresponding to the grey box) is shown in Fig. 5.
417

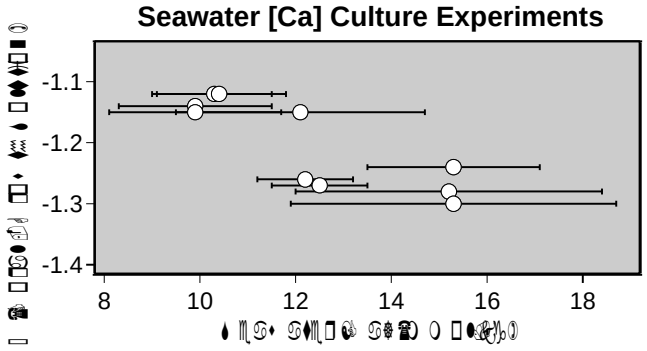

418

419 **Figure 5.** Enlargement of grey box from Fig. 4 showing the apparent fractionation
420 between culture solution and coral skeleton for experiments at modern and elevated
421 seawater [Ca]. Saturation state in the experiments also varied. Saturation states for
422 individual experiments are listed in Table 3.
423
424

To evaluate the hypothesis that coral Ca isotope fractionation may be sensitive to seawater [Ca], we measured Ca isotopes in cultured corals grown in solutions with [Ca] ranging from ~10 to ~15 mmol/kg (Table 3). The apparent fractionation between growth solution and coral skeleton for cultured corals is plotted against growth solution [Ca] in Fig. 5. We find that corals cultured at ~15 mmol/kg show a ~0.15‰ increase in Ca isotope discrimination relative to modern controls. This change in discrimination for cultured corals is in the same direction, but of slightly smaller magnitude, than the change we observe for fossil corals; given the fossil coral relationship, we would have expected a ~0.3 ‰ increase (Figs. 4 and 5). Overall, the growth experiment results give some support for our [Ca] hypothesis. However, additional experiments covering the full natural range of seawater [Ca] since the Mesozoic are necessary to confirm the proposed relationship. Although other seawater properties ([Mg] and [Sr]) were also varied in some of the experimental cases, we see no relationship between our cultured coral $\delta^{44/40}$Ca and these properties (see supplementary materials, Fig. S2).

Table 3 Results of Ca isotope analyses in cultured *Pocillopora damicornis*. Each sample represents the average offset between pairs of seawater solution, and the coral that was grown in that solution. Uncertainties are reported as 2σ S.D. where the number of replicate analyses (n) is = 2, and 2σ S.E. where n > 2.

Sample Name	$[Ca]_{seawater}$ (mmol/kg)	2σ S.D.	Ω	$\delta^{44/40}$Ca Offset *(coral - seawater)*	2σ S.D. /S.E.	n	Other modifications to culture solution
Control	10.3	1.2	2.3	-1.12	0.13	3	-
Control_Sr	9.9	1.6	2.3	-1.14	0.29	3	culture solution [Sr] = 2x modern
Control_Mg100	9.9	1.8	2.1	-1.15	0.20	3	culture solution [Mg] = 57 mmol/kg
Control_Mg200	10.4	1.4	1.7	-1.12	0.14	2	culture solution [Mg] = 61 mmol/kg
25% Elevated Ca_Mg100	12.5	1	2.9	-1.27	0.03	2	culture solution [Mg] = 57 mmol/kg
25% Elevated Ca_Mg200	12.2	1	2.3	-1.26	0.09	3	culture solution [Mg] = 59 mmol/kg
25% Elevated Ca	12.1	2.6	2.7	-1.15	0.08	2	-
50% Elevated Ca_Mg100	15.2	3.2	3.0	-1.30	-	1	culture solution [Mg] = 59 mmol/kg
50% Elevated Ca_Mg200	15.3	3.4	3.1	-1.28	0.18	3	culture solution [Mg] = 63 mmol/kg
50% Elevated Ca	15.3	1.8	2.9	-1.24	0.11	4	-

445 In the following sections, we explore various mechanisms that may lead to the
446 hypothesized change in coral Ca isotope discrimination over million year timescales. We
447 focus on those that may be dependent on seawater [Ca] and/or pH because both [Ca] and
448 pH may influence calcification dynamics. These mechanisms include (1) changes in coral
449 calcification rates and other inorganic $CaCO_3$ precipitation effects, (2) changes in proton
450 pumping in exchange for Ca^{2+}, (3) changes in Rayleigh distillation dynamics, and (4)
451 changes in the steady-state Ca mass balance of the calcifying fluid (termed here, the
452 "leaky Ca model").
453
454 *4.3.1 Calcification rate and inorgangic $CaCO_3$ precipitation effects*
455 Carbonate precipitation experiments show that Ca isotope fractionation is
456 sensitive to calcification rate (Lemarchand et al., 2004; Tang et al., 2008; Gussone et al.,
457 2003), but different experiments give conflicting results for the $\delta^{44/40}$Ca-rate dependence.
458 The Tang et al. (2008) calibration for inorganic calcite shows an inverse relationship
459 between $\delta^{44/40}$Ca and calcification rate. For this relationship, an increase in coral $\delta^{44/40}$Ca
460 between the Mesozoic and present would suggest decreasing calcification rates over that
461 time. In contrast, the Gussone et al. (2003) calibration for inorganic aragonite and the
462 Lemarchand et al. (2004) calibration for calcite show a positive relationship between
463 calcification rate and $\delta^{44/40}$Ca. This relationship instead suggests increasing calcification
464 rates between the Mesozoic and present. Although the direction for the calcification rate
465 dependence differs between published inorganic precipitation experiments, all generally
466 show that the $\delta^{44/40}$Ca of inorganic calcium carbonate varies by up to 1.5‰ over a two
467 order of magnitude range in precipitation rate (Lemarchand et al. 2004; Gussone et al.

468 2003; Tang et al. 2008). This observation indicates that coral calcification rates would
469 have needed to vary significantly – by about a factor of 10 – between the Mesozoic and
470 today to generate the ~0.8‰ change in apparent fossil coral Ca isotope discrimination.
471 Such a large change in calcification rates since the Mesozoic seems unlikely.
472 As inferred from culture experiments, rates of coral aragonite growth seem to correlate
473 most strongly with the saturation state of seawater ($\Omega = [Ca]\times[CO_3^{2-}]/K_{sp}$) with respect to
474 aragonite (e.g., Marubini et al. 2008). While seawater pH and $[CO_3^{2-}]$ have increased
475 significantly since the Mesozoic (Zeebe, 2012) constraints from reconstructions of the
476 calcium carbonate compensation depth through time suggest that seawater Ω has not
477 changed significantly over this same time interval (Zeebe, 2012). As a result, we suggest
478 that changes in calcification rate probably cannot account for observed changes in fossil
479 coral $\delta^{44/40}$Ca since the Mesozoic.
480 In addition, although it is difficult to draw conclusions over geologic timescales
481 based on short-term culture experiments, a calcification rate dependence does not seem to
482 explain our cultured coral data. Although calcification rates in our culture experiments
483 (as calculated from the alkalinity anomaly method and normalized to buoyant weights)
484 are inversely related to culture [Ca] we find no significant relationship between coral
485 $\delta^{44/40}$Ca and calcification rate (see supplementary materials; Fig. S1).
486 Because the $[Ca^{2+}]/[CO_3^{2-}]$ ratio of seawater likely decreased by almost an order
487 of magnitude between the Mesozoic and today (Lowenstein et al. 2003; Horita et al.
488 2002; Hönisch et al. 2012; Zeebe et al. 2012), it is also important to consider the potential
489 for kinetic isotope effects related to changes in seawater chemistry. Results of Nielsen
490 and DePaolo (2013), show that the magnitude of Ca isotope fractionation in carbonates

491 increases with decreasing $[Ca^{2+}]/[CO_3^{2-}]$. However, this kinetic effect can explain neither
492 the magnitude nor direction of change in fossil coral $\delta^{44/40}Ca$. The Nielsen and DePaolo
493 (2013) dependence would predict a decrease in coral $\delta^{44/40}Ca$ between the Mesozoic and
494 today – opposite from our results. It also predicts a low sensitivity of this relationship for
495 seawater conditions, which is insufficient to explain the ~0.8 ‰ difference between
496 Mesozoic and modern coral samples.
497
498 *4.3.2 Changes in proton pumping – a dependence on external seawater pH*
499 Corals exchange protons for Ca^{2+} via Ca-ATPase in order to elevate their
500 internal 'calcifying fluid' pH and promote calcification (Al-Horani et al., 2003; Gaetani
501 et al., 2011). As a result, changes in external seawater pH may drive changes in the
502 fraction of Ca derived from seawater relative to the amount derived from active transport.
503 Ca isotope fractionation associated with Ca-ATPase is estimated to be between -1.0 and -
504 1.7‰ (De La Rocha and DePaolo, 2000; Gussone et al. 2006; Böhm et al. 2006). This
505 estimate is based on the isotope effect observed for modern coccolithophore calcite since
506 almost all calcium in coccolith calcite is thought to derive from active transcellular
507 transport (Gussone et al., 2006). If indeed there is a significant fractionation associated
508 with active transport, then variations in transport could drive changes in the Ca isotope
509 composition of the coral calcifying fluid.
510 A recent set of coral culture experiments with *Porites australiensis*, however,
511 suggests that a sensitivity of Ca-pumping to external pH may not be able to explain the
512 changes we observe in fossil coral $\delta^{44/40}Ca$ since the Mesozoic (Inoue et al. 2015). In the
513 experiments, the pH of growth solutions was varied from 7.4 to 8.1 by bubbling with

514 CO_2. $\delta^{44/40}Ca$ of cultured coral skeleton precipitated in the different pH treatments shows
515 no relationship with culture solution pH (Inoue et al. 2015).
516
517 *4.3.3 Rayleigh fractionation – a dependence on seawater [Ca]*
518 Rayleigh distillation could fractionate Ca isotopes in a manner dependent on
519 seawater [Ca]. The Rayleigh fractionation hypothesis proposes that as calcification
520 proceeds from a seawater-like 'calcifying fluid', element/Ca ratios, or isotope ratios,
521 become progressively enriched or depleted according to their partitioning behavior into
522 the solid phase. For example, Mg/Ca ratios become enriched and Sr/Ca ratios become
523 depleted (since the K_D for Sr/Ca > 1 and the K_D for Mg/Ca << 1) (Gaetani et al. 2011).
524 Aragonite is isotopically depleted in the heavy isotopes of Ca relative to seawater, so the
525 $\delta^{44/40}Ca$ of both coral aragonite and the residual fluid should become isotopically heavy
526 as calcification proceeds. In the Rayleigh framework, the degree of calcium drawdown
527 during precipitation is represented by the term f - defined as the fraction of Ca remaining
528 in the fluid. At an f of 1, the [Ca] of the fluid is equal to the original [Ca]. At an f of 0, all
529 of the calcium present in the original fluid has been consumed. If f – on average – has
530 remained constant since the Mesozoic, no change in coral $\delta^{44}Ca$ would be expected due
531 to Rayleigh fractionation. However, if f varied with time, coral Ca isotope discrimination
532 could have varied as well.
533 It is currently unclear what determines the amount of Ca remaining in the
534 calcifying fluid (f), but it is possible that this parameter depends on the original [Ca] in
535 the calcifying fluid. Here, we consider the specific case wherein we assume corals
536 precipitate a fixed mass of Ca from their calcifying fluids regardless of external seawater

537 [Ca]. We acknowledge that in reality, the extent of Ca drawdown may actually depend on
538 different factors, and that this scenario may not be representative. For example, it could
539 be that the corals precipitate $CaCO_3$ until a given calcifying fluid Ca concentration is
540 reached, or until a given saturation state is reached. The Rayleigh '*f*' has also been
541 hypothesized to be dependent on external seawater pH and/or alkalinity (Gagnon et al.,
542 2013). Such scenarios would yield different predictions for how *f* changes with variations
543 in external seawater [Ca], but we do not explore them here.

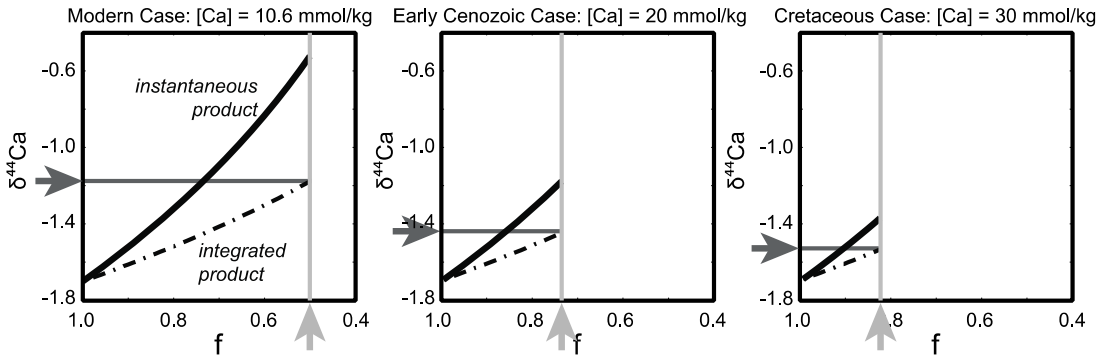

544

545 **Figure 6.** Results of Rayleigh fractionation calculations. The solid black line corresponds
546 to the instantaneous product and the black dashed line corresponds to the integrated
547 product of $\delta^{44/40}Ca$ in coral for the cases of modern, Early Cenozoic, and Cretaceous
548 seawater [Ca]. Modern *f* is assumed to be 0.5. The kinetic isotope effect for coral is
549 assumed to be the same as the isotope effect for inorganic aragonite, -1.7‰ (Gussone et
550 al., 2003; Blättler et al., 2012). The value for *f* for each seawater scenario is indicated
551 with the light gray arrows and is set by the requirement that the total mass of Ca
552 precipitated from each 'batch' of seawater during distillation remains constant. The value
553 for calculated coral $\delta^{44/40}Ca$ in each seawater scenario is indicated by the dark grey arrow
554 on the y-axis.
555

556 Fig. 6 shows plots of the instantaneous and integrated products of $\delta^{44/40}Ca$ in
557 coral under a Rayleigh fractionation scenario for modern, Early Cenozoic, and
558 Cretaceous seawater [Ca] conditions. The calculations used to generate each plot assume
559 a Ca drawdown of 5 mmol/L such that the total mass of Ca precipitated from each 'batch'
560 of seawater during distillation remains constant (as stated above) in each case. For the

561 modern scenario, where [Ca] in the calcifying fluid is assumed to be equal to modern
562 seawater ([Ca] = 10.6 mmol/L), the total fraction of Ca remaining in the calcifying fluid,
563 f, is 0.5. There have been a wide range of estimates for the value of coral f in the
564 literature. For example, Gagnon et al. (2007) suggest a value for deep-sea coral between
565 0.8 and 0.6. Cohen et al. (2009), on the other hand, suggest values much lower – close to
566 and f = 0.3. We choose a value of f = 0.5 as an intermediary value that is broadly
567 compatible with existing estimates. The isotope effect for coral aragonite precipitation is
568 set to be 1.7 ‰ - equal to the inorganic aragonite fractionation at 15°C (Gussone et al.,
569 2003; Blättler et al., 2012). Fossil and modern corals likely grew at warmer temperatures
570 (~25°C), such that a value of 1.6 ‰ is more appropriate, but small changes in the choice
571 of isotope effect do not greatly impact our calculations. We calculate that f shifts from a
572 value of 0.5 for the case of modern seawater [Ca] to a value of ~0.8 for Cretaceous
573 seawater [Ca]. This magnitude of change in f leads to a 0.34‰ depletion in the $\delta^{44/40}$Ca
574 integrated product between the modern and Cretaceous case. Instead, if an isotope effect
575 of 1.0 ‰ is chosen, we calculate a 0.20 ‰ depletion in the $\delta^{44/40}$Ca integrated product
576 between the modern and Cretaceous case. These magnitudes of change cannot account
577 for the full, 0.8‰ decrease in Ca isotope discrimination between the Mesozoic and today.
578 Thus, we conclude that a Rayleigh fractionation response to changes in seawater [Ca] can
579 contribute to the observed δ^{44}Ca increase in fossil corals, but cannot explain the entire
580 change.

581 It is important to note that the magnitude of change between the modern and
582 Cretaceous case for these scenarios significantly depends on the choice of f for the
583 modern scenario. If f is chosen to be 0.3 or 0.2, more consistent with values of Cohen et

584 al. (2009) and Gaetani et al. (2011), then we would calculate a ~0.6 ‰ decrease in Ca
585 isotope discrimination between the Cretaceous and present. While this value approaches
586 the ~0.8 ‰ decrease observed, it still cannot account for the entire change.
587
588 *4.3.4 The 'leaky calcium model' – a dependence on seawater [Ca]*
589 It is also possible that the calcifying fluid remains open to seawater and can be
590 modeled as a series of steady states with respect to Ca inputs and outputs (Fig. 7). In this
591 case, the isotopic composition of Ca precipitated from the calcifying fluid depends on: (1)
592 the exchange rate of Ca between seawater and the calcifying fluid relative to Ca
593 incorporation into the coral skeleton, and (2) the isotope effects associated with each
594 pathway. We call this model the 'leaky calcium model'. Calcium isotope discrimination
595 in this framework can be likened to carbon isotope discrimination by RuBisCO in plants
596 – the magnitude of which is dependent on atmospheric CO_2 concentrations (Pagani,
597 2014).
598

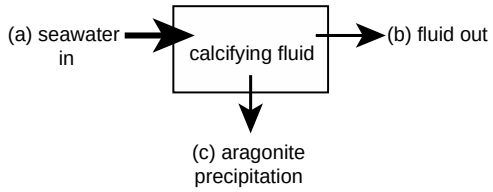

599
600 **Figure 7.** Schematic showing the steady state Ca mass balance of the coral calcifying
601 fluid.
602
603 We assume that Ca is sourced to the calcifying fluid by direct transport of
604 seawater, and that contributions from Ca-ATPase are minimal (see Section 4.3.2; Figs. 1

and 7). Ca is removed by skeletal precipitation or by advective or diffusive transport back to seawater. As in the previous section, we also assume that the isotope effect associated with skeletal precipitation from the calcifying fluid is equal to the fractionation factor for inorganic aragonite, 1.7‰ (Gussone et al., 2003; Blättler et al., 2012). Following expressions for carbon isotope fractionation by RuBisCo (Pagani, 2014), we express Ca isotope fractionation for this system as follows:

$$\Delta_{Coral\text{-}Arag} = \varepsilon_{transport} + (\varepsilon_{ppt} - \varepsilon_{transport}) \times F \qquad \text{(Eqn. 2)}$$

where $\varepsilon_{transport}$ represents the isotope effect associated with transport of Ca from seawater to the calcifying fluid, ε_{ppt} is the isotope effect associated with skeletal precipitation, F represents the fraction of Ca that is transported back to seawater from the calcifying fluid, and $\Delta_{Coral\text{-}Arag}$ is the total fractionation expressed in the coral skeleton. We assume that no isotope effect occurs during transport of seawater into the calcifying space, such that $\varepsilon_{transport} = 0$.

If the mass of $CaCO_3$ precipitated from the calcifying fluid is constant, $\Delta_{Coral\text{-}Arag}$ will increase at higher seawater [Ca] because a greater fraction of Ca will be transported back to seawater relative to the total amount of Ca in the calcifying fluid. In other words, F will increase as seawater [Ca] increases. Alternatively, we can write a steady state equation for the 'leaky calcium' scenario (see supplementary for full derivation):

$$R^{44/40}Ca_{coral} = (\alpha \times R^{44/40}Ca_{seawater})/(F + \alpha \times (1 - F)), \qquad \text{(Eqn. 3)}$$

where *F* is the fraction of Ca that exits the calcifying fluid and is transported back to seawater (Fig. 7, *b*) relative to the amount transported in (Fig. 7, *a*). If coral aragonite precipitation occurs over a series of steady states ranging from *F = 1* to *F = 0.5* (for the modern scenario) or *F = 1* to *F = 0.8* (for the Cretaceous case – as assumed in Section 4.2.3), then we can integrate over Eqn. 3 to calculate a change in Ca isotope discrimination in the bulk coral skeleton. This calculation produces results of the same magnitude as the Rayleigh model: a ~0.25‰ depletion in the integrated product between the modern (*F = 0.5*) and Cretaceous case (*F = 0.8*). We conclude as above, that the 'leaky Ca model' can contribute to the observed $\delta^{44/40}$Ca increase in fossil corals, but cannot explain the entire change.

5. Conclusions

Fossil corals are important archives of paleoclimatic and paleoenvironmental change, but vital effects can obscure, or lead to inaccuracies in coral-based environmental reconstructions. Here, we present measurements of $\delta^{44/40}$Ca in a suite of extremely well preserved aragonitic fossil corals that, together with data from bulk pelagic carbonates, indicate coral Ca isotope discrimination may have decreased by ~0.8‰ between the Mesozoic and today. We propose that the decrease in discrimination, going forward in time, could result from a vital effect of calcification. Specifically, we suggest that biomineralization dynamics respond to secular variations in seawater [Ca]. Culture experiments that test for the dependence of coral $\delta^{44/40}$Ca on growth solution [Ca] lend some support for this hypothesis. However, additional experiments are necessary to

confirm the sensitivity over the natural range of seawater [Ca] for the Mesozoic and Cenozoic. Changes in Rayleigh fractionation, or a 'leaky Ca model' may be able to explain part, but not all, of the apparent change. Our results provide geochemical constraints on models of coral biomineralization, and emphasize the importance of understanding the mechanisms driving vital effects in biogenic carbonates that are used to reconstruct ancient environmental properties.

Acknowledgements

We would like to thank Stephen Cairns and Tim Coffer (Smithsonian Institution), Linda Ivany (Syracuse University), Roger Portell (Florida Museum of Natural History), Anne Cohen and Bill Thompson (WHOI), the USGS, and Gregory Dietl (Paleontological Research Institution) for loaning samples. We would also like to thank Alex Gagnon for helpful discussions and Elizabeth Lundstrom for analytical assistance. We would like to acknowledge the Princeton BP Amoco Carbon Mitigation Initiative and the Frank Harrison Tuttle Memorial Fund for Invertebrate studies for their generous support.

References

Al-Horani, F.A., Al-Moghrabi, S.M., de Beer, D., 2003. The mechanism of calcification and its relation to photosynthesis and respiration in the scleractinian coral *Galaxea fascicularis*. *Marine Biology* 142, 419-426.

Barker, P.F., Johnson, D.A., Carlson, R.L., et al. 1983. Site 516; Rio Grande Rise, DSDP

674 Deep Sea Drilling Project.
675 Blättler, C.L., Henderson, G.M., Jenkyns, H.C., 2012. Explaining the Phanerozoic Ca isotope
676 history of seawater. *Geology* 40, 843-846.
677 Blättler, C.L., Higgins, J.A., 2014. Calcium isotopes in evaporites record variations in
678 Phanerozoic seawater SO_4 and Ca. *Geology* 42, 711-714.
679 B□hm, F., N. Gussone, A. Eisenhauer, W-C. Dullo, S. Reynaud, A. Paytan, 2006. Calcium
680 isotope fractionation in modern scleractinian corals. *Geochimica et Cosmochimica Acta*
681 70, 4452-4462.
682 Chang, V.T.-C., Williams, R.J.P., Makishima, A., Belshawl, N.S., O'Nions, R.K., 2004. Mg
683 and Ca isotope fractionation during $CaCO_3$ biomineralisation. *Biochemical and*
684 *Biophysical Research Communications* 323, 79-85.
685 Cohen, A.L., McCorkle, D.C., de Putron, S., Gaetani, G.A., Rose, K.A. (2009)
686 Morphological and compositional changes in the skeletons of new coral recruits reared
687 in acidified seawater: Insights into the biomineralization response to ocean
688 acidification. *Geochemistry, Geophysics, Geosystems* 10, Q07005.
689 Corrège, T., 2006. Sea surface temperature and salinity reconstruction from coral
690 geochemical tracers. *Palaeogeography, Palaeoclimatology, Palaeoeclogy* 232, 408-
691 428.
692 De La Rocha, C.L., DePaolo, D.J., 2000. Isotopic Evidence for Variations in the Marine
693 Calcium Cycle Over the Cenozoic. *Science* 289, 1176-1178.
694 Fantle, M.S., DePaolo, D.J., 2005. Variations in the marine Ca cycle over the past 20 million
695 years. *Earth and Planetary Sciences* 237, 102-117.

696 Fantle, M.S., DePaolo, D.J., 2007. Ca isotopes in carbonate sediment and pore fluid from
697 ODP Site 807A: The Ca^{2+}(aq)-calcite equilibrium fractionation factor and calcite
698 recrystallization rates in Pleistocene sediments. *Geochimica et Cosmochimica Acta* 71,
699 2524-2546.
700 Fantle, M.S., Maher, K.M., DePaolo, D.J., 2010. Isotopic approaches for quantifying the
701 rates of marine burial diagenesis. *Reviews of Geophysics* 48, RG3002.
702 Fantle, M.S., Higgins, J.A., 2014. The effects of diagenesis and dolomitization on Ca and Mg
703 isotopes in marine platform carbonates: Implications for the geochemical cycles of Ca
704 and Mg. *Geochimica et Cosmochimica Acta* 142, 458-481.
705 Fantle, M.S., Tipper, E.T., 2014. Calcium isotopes in the global biogeochemical Ca cycle:
706 Implications for development of a Ca isotope proxy. *Earth-Science Reviews* 129, 148-
707 177.
708 Farkaš, J., Böhm, F., Wallmann, K., Blenkinsop, J., Eisenhauer, A., van Geldern, R.,
709 Munnecke, A., Voigt, S., Veizer, J., 2007. Calcium isotope record of Phanerozoic
710 oceans: Implications for chemical evolution of seawater and its causative mechanisms.
711 *Geochimica et Cosmochimica Acta* 71, 5117-5134.
712 Gaetani, G.A., Cohen, A.L., Wang, Z., Crusius, J., 2011. Rayleigh-based, multi-element
713 coral thermometry: A biomineralization approach to developing climate proxies.
714 *Geochimica et Cosmochimica Acta* 75, 1920-1932.
715 Gagnon, A.C., Adkins, J.F., Erez, J., Eiler, J.M., Guan, Y., 2013. Sr/Ca sensitivity to
716 aragonite saturation state in cultured subsamples from a single colony of coral:
717 Mechanism of biomineralization during ocean acidification. *Geochimica et*
718 *Cosmochimica Acta* 105, 240-254.

719 Gagnon, A.C., Adkins, J.F., Fernandez, D.P., Robinson, L.F., 2007. Sr/Ca and Mg/Ca vital
720 effects correlated with skeletal architecture in a scleractinian deep-sea coral and the role
721 of Rayleigh fractionation. *Earth and Planetary Science Letters,* 261, 280-295.
722 Griffith, E.M., Paytan, A., Caldeira, K., Buillen, T.D., Thomas, E., 2008. A dynamic marine
723 calcium cycle during the past 28 million years. *Science* 3322, 1671-1674.
724 Gothmann, A.M., Stolarski, J., Adkins, J.F., Dennis, K.J., Schrag, D.P., Schoene, B., Bender,
725 M.L., 2015. Fossil corals as an archive of secular variations in seawater chemistry.
726 *Geochimica et Cosmochimica Acta*.
727 Gussone, N., Eisenhauer, A., Heuser, A., Dietzel, M., Bock, B., Böhm, F., Spero, H., Lea, D.,
728 Bijma, J., Nägler, T.F., 2003. Model for kinetic effects on calcium isotope fractionation
729 δ^{44}Ca in inorganic aragonite and cultured planktonic foraminifera. *Geochimica et*
730 *Cosmochimica Acta* 67, 1375-1382.
731 Gussone, N., Langer, G., Thoms, S., Nehrke, G., Eisenhauer, A., Riebesell, U., Wefer, G.,
732 2006. Cellular calcium pathways and isotope fractionation in *Emiliana huxleyi*.
733 *Geology* 34, 625-628.
734 Heuser, A., Eisenhauer, A., 2008. The Calcium Isotope Composition ($\delta^{44/40}$Ca) of NIST SRM
735 915b and NIST SRM 1486. *Geostandards and Geoanalytical Research* 32, 311-315.
736 Heuser, A., Eisenhauer, A., Böhm, F., Wallmann, K., Gussone, N., Pearson, P.N., Nägler,
737 T.F., Dullo, W., 2005. Calcium isotope $\delta^{44/40}$Ca variations of Neogene planktonic
738 foraminifera. *Paleoceanography* 20.
739 Higgins, J.A., Schrag, D.P., 2015. The Mg isotopic composition of Cenozoic seawater -
740 evidence for a link between Mg-clays, seawater Mg/Ca, and climate. *Earth and*
741 *Planetary Science Letters* 416, 73-81.

742 Holmden, C., Papanastassiou, D.A., Blanchon, P., Evans, S., 2012, $\delta^{44/40}$Ca variability in
743 shallow water carbonates and the impact of submarine groundwater discharge on Ca-
744 cycling in marine environments. *Geochimica et Cosmochimica Acta* 83, 179-194.
745 Hönisch, B., Ridgwell, A., Schmidt, D.N., Thomas, E., Gibbs, S.J., Sluijs, A., Zeebe, R.E.,
746 Kump, L., Martindale, R.C., Greene, S.E., Kiessling, W., Ries, J., Zachos, J.C., Royer,
747 D.L., Barker, S., Marchitto Jr., T.M., Moyer, R., Pelejero, C., Ziveri, P., Foster, G.L.,
748 Williams, B., 2012. The Geological Record of Ocean Acidification. *Science* 335, 1058-
749 1063.
750 Inoue, M., Gussone, N., Koga, Y., Iwase, A., Suzuki, A., Sakai, K., Kawahata, H., 2015.
751 Controlling factors of Ca isotope fractionation in scleractinian corals evaluated by
752 temperature, pH and light controlled culture experiments. *Geochimica et Cosmochimica*
753 *Acta* 167, 80-92.
754 Kisakürek, B., A., Eisenhauer, A., Bohm, A., Hathorne, E.C., Erez, J., 2011. Controls on
755 calcium isotope fractionation in cultured planktic foraminifera, *Globigerinoides ruber*
756 and *Globigerinella siphonifera*. *Geochimica et Cosmochimica Acta* 75, 427-443.
757 Kroenke, L.W., Berger, W.H., Janecek, T.R., et al., (1991) *Proceedings of the Ocean*
758 *Drilling Program, Initial Reports, Vol. 130*.
759 Lehn, G., Jacobson, A.D., Holmden, C., 2013. Precise analysis of Ca isotope ratios ($\delta^{44/40}$Ca)
760 using an optimized ^{43}Ca-^{42}Ca double-spike MC-TIMS method. *International Journal of*
761 *Mass Spectrometry* 351, 69-75.
762 Lemarchand, D., Wasserburg, G.J., Papanastassiou, D.A., 2004. Rate-controlled calcium
763 isotope fractionation in synthetic calcite. *Geochimica et Cosmochimica Acta* 68, 4665-
764 4678.

765 Lowenstein, T.K., Hardie, L.A., Timofeeff, M.N., Demicco, R.V., 2003. Secular variation in
766 seawater chemistry and the origin of calcium chloride basinal brines. *Geology* 31, 857-
767 860.
768 Marubini, F., Ferrier-Pagès, C., Furla, P., Allemand, D., 2008. Coral calcification responds to
769 seawater acidification: a working hypothesis towards a physiological mechanism. *Coral*
770 *Reefs* 27, 491-499.
771 McCulloch, M.T., Trotter, J., Montagna, P., Falter, J., Dunbar, R., Freiwald, A., Forsterra,
772 G., Lopez Correa, M., Maier, C., Ruggeberg, A., Taviani, M., 2012. Resilience of cold-
773 water scleractinian corals to ocean acidification: Boron isotopic systematics of pH and
774 saturation state up-regulation. *Geochimica et Cosmochimica Acta* 87, 21-34.
775 Milliman, J.D., 1993. Production and accumulation of calcium carbonate in the ocean:
776 Budget of a nonsteady state. *Global Biogeochemical Cycles* 7, 927-957.
777 Morgan, J.L.L., Gordon, G.W., Arrua, R.C., Skulan, J.L., Anbar, A.D., Bullen, T.D., 2011.
778 High-precision measurement of variations in calcium isotope ratios in urine by multiple
779 collector inductively coupled plasma mass spectrometry. *Analytical Chemistry* 83,
780 6956-6962.
781 Nielsen, L.C. and DePaolo, D.J., 2013. Ca isotope fractionation in a high-alkalinity lake
782 system: Mono Lake, California. *Geochimica et Cosmochimica Acta* 118, 276-294.
783 Pagani, M., 2014. Biomarker-Based Inferences of Past Climate: The Alkenone pCO_2 Proxy,
784 in: Treatise on Geochemistry (second edition). Holland, H.D., Turekian, K.K. (Eds.),
785 Elseiver, Oxford, pp. 361-378.
786 Pretet, C., Samankassou, E., Felis, T., Reynaud, S., Böhm, F., Eisenhauer, A., Ferrier-Pagès,
787 C., Gattuso, J., Camoin, G., 2013. Constraining calcium isotope fractionation ($\delta^{44/40}Ca$)

788 in modern and fossil scleractinian coral skeleton. *Chemical Geology* 340, 49-58.
789 Schmitt, A.-D., P. Stille, and T. Vennemann, 2003. Variations of the $^{44}Ca/^{40}Ca$ ration in
790 seawater during the past 24 million years: Evidence from $\delta^{44}Ca$ and $\delta^{18}O$ values of
791 Miocene phosphates. *Geochimica et Cosmochimica Acta* 67, 2607-2614.
792 Sime, N.G., C. L. De La Rocha, E. T. Tipper, A. Tripati, A. Galy, M. J. Bickle, DeLarocha,
793 C.L., Tipper, E.T., A. Galy, J. Gaillardet, M. J. Bickle, H. Elderfield, E. Carder, Tripati,
794 A.K., Galy, A., Bickle, M.J., 2007. Interpreting the Ca isotope record of marine
795 biogenic carbonates. *Geochimica et Cosmochimica Acta* 71, 3979-3989.
796 Soudry, D., Segal, I., Nathan, Y., Glenn, C.R., Halicz, L., Lewy, Z., VoderHaar, D.L., 2004.
797 $^{44}Ca/^{42}Ca$ and $^{143}Nd/^{144}Nd$ isotope variations in Cretaceous-Eocene Tethyan francolites
798 and their bearing on phosphogenesis in the southern Tethys. *Geology* 32, 389-392.
799 Soudry, D., Glenn, c.R., Nathan, Y., Segal, I., VoderHaar, D.L., 2006. Evolution of Tethyan
800 phosphogenesis along the northern edges of the Arabian-African shield during the
801 Cretaceous-Eocene as deduced from temporal variations of Ca and Nd isotopes and
802 rates of P accumulation. *Earth-Science Reviews* 78, 27-57.
803 Steuber, T., Buhl, D., 2006. Calcium-isotope fractionation in selected modern and ancient
804 marine carbonates. *Geochimica et Cosmochimica Acta* 70, 5507-5521.
805 Tambutte, E., Tambutte, S. Segonds, N. Zoccola, D., Venn, A., Erez, J., Allemand, D., 2011.
806 Calcein labelling and electrophysiology: insights on coral tissue permeability and
807 calcification. *Proceedings of the Royal Society B,* DOI: 10.1098/rspb.2011.0733.
808 Tang, J., Dietzel, M., Bohm, A., Kohler, P., Eisenhauer, A., 2008. Sr^{2+}/Ca^{2+} and $^{44}Ca/^{40}Ca$
809 fractioning during inorganic calcite formation: II. Ca isotopes. *Geochimica et*
810 *Cosmochimica Acta* 72, 3733-3745.

Venn, A.A., Tambutté, E., Holcomb, M., Laurent, J., Allemand, D., Tambutté, S., 2013. Impact of seawater acidification on pH at the tissue-skeleton interface and calcification in reef corals. *Proceedings of the Nationatal Academy of Sciences* 110, 1634-1639.

Weiner, S., Dove, P.M., 2003. An Overview of Biomineralization Processes and the Problem of the Vital Effect. *Reviews in Mineralogy and Geochemistry* 54, 1-29.

Zeebe, R.E., 2012. History of Seawater Carbonate Chemistry, Atmospheric CO_2, and Ocean Acidification. *Annual Review of Earth and Planetary Sciences* 40, 141-165.

Table Captions

Table 1. Results of Ca isotope analyses in Recent and fossil corals. Uncertainties are reported as 2σ S.D. where the number of replicate analyses (n) is = 2, and 2σ S.E. where n > 2. Ages are based on $^{87}Sr/^{86}Sr$ isotope compositions or best estimates of the age of the geologic formation from which samples are collected as detailed in Gothmann et al. (2015).

Table 2. Results of Ca isotope analyses on bulk carbonates from deep sea sediments. Ages are based on biostratigraphic markers at the depth from which the sample was

collected (Barker et al. 1983; Kroenke et al. 1991). Uncertainties are reported as 2σ S.D. where the number of replicate analyses (n) is = 2, and 2σ S.E. where n > 2.

Table 3. Results of Ca isotope analyses in cultured *Pocillopora damicornis*. Each sample represents the average offset between pairs of seawater solution, and the coral that was grown in that solution. Uncertainties are reported as 2σ S.D. where the number of replicate analyses (n) is = 2, and 2σ S.E. where n > 2.

Figure Captions

Figure 1. Sketch of key skeletal compartments and reservoirs that play a role in coral calcification, modified from Böhm et al. (2006). Seawater transport to the site of calcification can occur via direct exchange, or can occur transcellularly by active transport with Ca-ATPase. The label 'c' denotes arrows marking calcification.

Figure 2. Records of inferred seawater, fossil coral, and bulk pelagic carbonate Ca isotopes. (a) Records of inferred seawater $\delta^{44/40}$Ca vs. time including our record from fossil corals. Evaporite data are from Blättler and Higgins, (2014); brachiopods, belemnites and rudists are from Farkaš et al. (2007) and Steuber and Buhl (2006); phosphate data are from Soudry et al. (2004), Soudry et al. (2006) and Schmitt et al. (2003); barite data are from Griffith et al. (2008); foraminifera data are from Sime et al. (2007) and Heuser et al. (2005). (b) Same as in (a), but enlarged to show only the last 40 Myr. Uncertainties in fossil coral $\delta^{44/40}$Ca are listed in Table 1. Before the Late Eocene,

857 fossil corals disagree with other archives, with the exception of authigenic phosphates.
858 The left-hand axis gives inferred seawater $\delta^{44/40}$Ca compositions. The right-hand axis
859 gives measured coral $\delta^{44/40}$Ca vs. modern seawater. (c) Records of bulk carbonates from
860 this study (ODP Site 807 and DSDP Site 516), Fantle and DePaolo (2005), and Fantle
861 and DePaolo (2007). All records are normalized to modern bulk carbonate samples.
862
863 **Figure 3.** Models of the evolution of seawater and bulk carbonate $\delta^{44/40}$Ca in response to
864 perturbations in the isotopic composition of Ca inputs and the isotopic fractionation
865 associated with the carbonate output. (a) Response of seawater $\delta^{44/40}$Ca to a 0.15 ‰ step
866 increase in the $\delta^{44/40}$Ca of rivers (the main Ca input to seawater) going forward in time,
867 and (b) the response of bulk carbonate $\delta^{44/40}$Ca for the same perturbation. (c) Response of
868 seawater $\delta^{44/40}$Ca to a 1 ‰ change in ε – the isotopic fractionation associated with the
869 carbonate output, and (d) the response of bulk carbonate $\delta^{44/40}$Ca for the same
870 perturbation. Note the transient response in the $\delta^{44/40}$Ca of the bulk carbonate output,
871 which recovers to initial values as per the residence time of Ca (~1 My).
872
873 **Figure 4.** Fossil and cultured coral Ca isotope discrimination against seawater [Ca].
874 Black filled circles correspond to fossil coral samples. Estimates for seawater [Ca]
875 corresponding to each fossil coral sample are derived from reconstructions from fluid
876 inclusions in halite (Lowenstein et al. 2003; see supplementary materials for more detail).
877 White circles correspond to corals grown in culture experiments, which were performed
878 across a range of culture solution [Ca] concentrations. An enlargement of the culture
879 coral data (region corresponding to the grey box) is shown in Fig. 5.

Figure 5. Enlargement of grey box from Fig. 4 showing the apparent fractionation between growth solution and coral skeleton for experiments at modern and elevated seawater [Ca]. Saturation state in the experiments also varied. Saturation states for individual experiments are listed in Table 3.

Figure 6. Results of Rayleigh fractionation calculations. The solid black line corresponds to the instantaneous product and the black dashed line corresponds to the integrated product of $\delta^{44}Ca$ in coral for the cases of modern, Early Cenozoic, and Cretaceous seawater [Ca]. Modern *f* is assumed to be 0.5. The equilibrium isotope effect for coral is assumed to be the same as the isotope effect for inorganic aragonite, -1.7‰ (Gussone et al., 2005; Blättler et al., 2012). The value for *f* for each seawater scenario is indicated with the light gray arrows and is set by the requirement that the total mass of Ca precipitated from each 'batch' of seawater during distillation remains constant. The value for calculated coral $\delta^{44}Ca$ in each seawater scenario is indicated by the dark grey arrow on the y-axis.

Figure 7. Schematic showing the steady state Ca mass balance of the coral calcifying fluid.